CHANNELS AND FOSSAE EAST OF OLYMPUS MONS AS INDICATORS OF LATE AMAZONIAN VOLCANIC, HYDROLOGICAL, AND TECTONIC PROCESSES. S. S. Sutton[1], C. W. Hamilton[1], V. Cataldo[2], D. A. Williams[2], and J. E. Bleacher[3], [1]Lunar and Planetary Laboratory, University of Arizona, Tucson, AZ, USA (ssutton@lpl.arizona.edu), [2]School of Earth and Space Exploration, Arizona State University, Tempe, AZ, [3]Planetary Geology, Geophysics, and Geochemistry Laboratory, NASA Goddard Space Flight Center, Greenbelt, MD, USA.

Introduction: The formation of sinuous channels in the Tharsis Volcanic Province has been attributed to lava [1–3], aqueous flows [1,4,5], or a combination of both volcanic and aqueous processes [6]. To investigate the question of whether the channels were formed by flowing lava or by liquid water, we conducted a detailed geomorphological study of two representative regions featuring sinuous channels and associated fossae located within the Late Amazonian volcanic plains east of Olympus Mons [7]. We mapped the distribution of channels, fossae, vents, and small shields within the larger context area, and constructed a relative sequence of the geologic history at two sites, designated as the northwest (NW) and southeast (SE) regions (**Fig. 1**). Within these regions, we classified channels and fossae into types based on morphology, calculated the potential for lava to achieve turbulent flow in this setting, and interpreted the results to assess the relationship between volcanic, tectonic, and hydrological processes in the vicinity east of Olympus Mons.

Data: The primary data sets used in the geomorphological mapping of the NW and SE regions were images from the High Resolution Imaging Science Experiment (HiRISE) [8] and Context Camera (CTX) [9], and digital terrain models (DTMs) derived from HiRISE and CTX stereo pairs following the methods of [10]. Regional topographic analyses were performed on the Mars Orbiter Laser Altimeter (MOLA) global Mission Experiment Gridded Data Record (MEGDR) [11]. An uncontrolled CTX mosaic was created to map geologic units and structures in the context area from 11.0º–23.0º N and 228.0º–238.5º E.

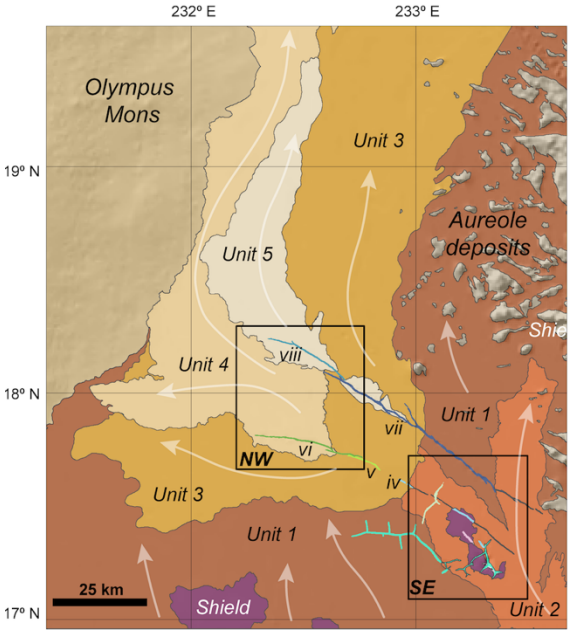

Figure 1. Map of stratigraphic relationships of flow units and fossae for the NW and SE regions (black rectangles) and surrounding area.

Geomorphological Mapping: We identified five major flow units and eight fossae systems spanning the NW and SE regions and vicinity. From our mapping of the superposition of flow units and fossae, we ascertained the relative sequence of geologic activity in the area encompassing our two focused study sites (**Fig. 1**). Within *Unit 4* in the NW region, and *Unit 2* in the SE region, we mapped flow units, channels, fossae, and vents in detail.

Based on their morphologic characteristics, we classified the channels into three types (*Channel Type 1*, *2*, and *3*), and the fossae into two types (*Fossae Type L* and *A*). *Channel Type 1* and *Type 2* display constructional characteristics consistent with volcanic origin, including rough and irregular margins with leveed banks, rectilinear cross-sectional profiles, and marginal lobate flows [12,13]. Diagnostic morphologies of *Type 3* channels include cut bank erosion, smooth, shallow banks, and streamlined features [14,15]. *Channel Type 3* morphology is consistent with aqueous erosion by a hyperconcentrated debris flow [16–18].

Fossae Type L are deeply incised linear graben or troughs with en echelon segments. *Fossae Type A* have branched, arcuate segments that form steep-sided troughs. We interpret that *Fossae Type L* are the surface expressions of dike intrusion [19]. *Type A* fossae geometry may be due to topographic updoming and surface fracturing resulting from sill emplacement [20–22]. Aqueous erosion of channels co-located with the *Type A* fossae system in the SE region implies groundwater release. Sill formation could have provided a sufficient heat source to initiate melting of buried ice deposits.

Lava Turbulence Modeling: To test the possibility that the channels were formed by lava erosion, we calculated the likelihood that lava could flow turbulently within the rheological parameters consistent with the physical boundary conditions set by the topography and morphology of the channels and associated flow units. Our calculations for the NW

region show that fully turbulent flow could only have been reached within the range of measured channel depths for the very low-viscosity cases (<50 Pa s). In the SE region, fully turbulent flow was not achieved for any of the cases within the range of measured channel depths. Our calculations show that for reasonable rheological parameters, turbulent lava flow (i.e., lava flows with the most potential to erode [23–25]) would be least likely in the SE region, although this is where the signatures of erosive morphology are prevalent.

Implications for Volcanic, Hydrological, and Tectonic Activity: The history of the area encompassing the NW and SE regions is of an ongoing, distributed, monogenetic style of volcanism. The presence of fossae and channels in the Late Amazonian volcanic plains points to a widely distributed magma source region feeding dikes and sills that alternately released eruptions of sheet flows (dikes) (e.g., [26]), or provided localized heat sources (sills) that could have released melted subsurface ice, causing hyperconcentrated aqueous flows at the surface.

Olympus Mons produces downward stress on the lithosphere at the center of the edifice, transitioning to horizontal compressive stresses near the basal scarp [27,28]. Throughout the growth of Olympus Mons, the orientation of the least compressive stress within the flexural moat [29] may have alternately favored sill or dike formation. After strain release due to radial normal or strike-slip faulting, dike emplacement is favored until additional loading develops compression again, favoring sill emplacement (**Fig. 2**). We attribute the formation and distribution of channels and fossae throughout the plains east of Olympus Mons to be a consequence of the region's evolving states of stress, which are predominantly influenced by the loading of Olympus Mons.

Acknowledgments: This research was funded in part by NASA Planetary Geology and Geophysics, USA Grant NNX14AL54G to CWH, DAW, and JEB, and by the National Science Foundation Graduate Research Fellowship Grant DGE-1746060 to SSS. HiRISE DTMs created for this work are available in the PDS and at https://uahirise.org/dtm.

References: [1] Mouginis-Mark, P.J. and Christensen, P.R. (2005) *JGR, 110*. [2] Garry, W.B., Zimbelman, J.R., Gregg, T.K.P. (2007) *JGR, 112*. [3] Bleacher J.E. et al. (2017) *JVGR, 342*. [4] Mouginis-Mark, P.J. (1990) *Icarus, 84*. [5] Basilevsky, A.T. et al. (2006) *GRL, 33*(13). [6] Hargitai, H.I. and Gulick V.C. (2018) in *Dynamic Mars*. [7] Sutton, S.S. et al. (2022) *Icarus, 374*. [8] McEwen, A.S. et al. (2007) *JGR, 112*. [9] Malin, M.C. et al. (2007) *JGR, 112*. [10] Kirk, R.L. et al. (2008) *JGR, 113*. [11] Smith, D.E. et al. (2001) *JGR, 106*. [12] Lipman, P.W. and Banks, N.G. (1987) in *USGS Prof. Paper 1350*. [13] Harris, A.J.L. et al. (2009) *Bull. Volc., 71*. [14] Bridge, J.S. (1977) *Earth Surf. Proc., 2*(4). [15] Wohl, E.E. (1993) *Aust. J. Geol., 101*(6). [16] Baker, V. (1973) in *Fluvial Geomorphology*. [17] Fagents, S.A. and Baloga, S.M. (2006) *JGR, 111*(10). [18] Doyle, E.E., Cronin, S.J., Thouret, J.C. (2011) *Bull. GSA, 123*(7–8). [19] Rubin, A.M. (1992) *JGR, 97*(91). [20] Koide, H. and Bhattacharji, S. (1975) *Econ. Geol., 70*(4). [21] Pollard, D.D. and Johnson, A.M. (1973) *Tectonophys., 18*(3–4). [22] Pollard, D.D. and Holzhausen, G. (1979) *Tectonophys., 53*(1–2). [23] Hulme, G. (1982) *Geophys. Surv., 5*(3). [24] Huppert, H.E. (1989) *J. Fluid Mech., 198*. [25] Williams, D.A. et al. (1998) *JGR, 103*(B11). [26] Muirhead, J.D. et al. (2014) *EPSL, 406*. [27] McGovern, P.J. and Solomon, S.C. (1993) *JGR, 98*(93). [28] Musiol, S. et al. (2016) *JGR, 121*(3). [29] McGovern, P.J. et al. (2002) *JGR, 107*.

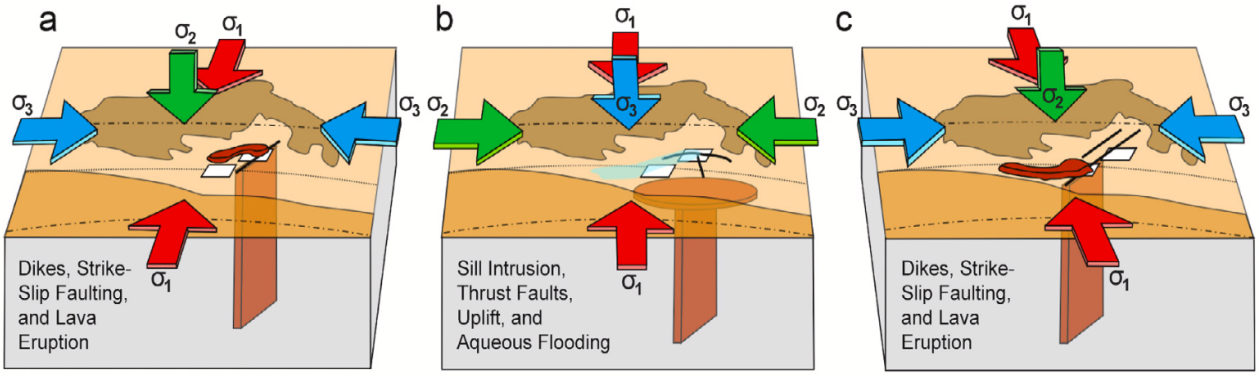

Figure 2. Schematic of alternating regional stress states. The view in perspective is from Olympus Mons looking east. The directions of the three principal stresses ($\sigma^1 > \sigma^2 > \sigma^3$), are indicated by the red, green, and blue arrows, respectively.